Geochemical Perspectives Letters

Modelling redox state *via* V-Sc-Ti-Yb partitioning in mantle derived melts

C.-T. Liu[1*], C.-Y. Ye,[1], J. ZhangZhou[1*]

OPEN ACCESS

https://doi.org/10.7185/geochemlet.2504

Abstract

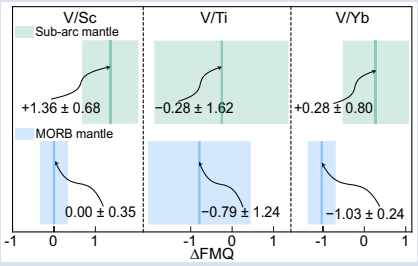

The ratios of multivalent V to homovalent elements (*e.g.*, V/Sc, V/Ti, V/Yb) are pivotal proxies for assessing mantle oxygen fugacity (fO_2), yet their geochemical behaviours during partial melting remain debatable. Here, we conducted petrological modelling to explore the responses of these ratios to fO_2 variations in sub-arc and mid-ocean ridge basalt (MORB) mantle sources, considering diverse mineral assemblages and chemical compositions. Our results suggest that V/Sc is relatively unaffected by changes in mantle source characteristics and melting extent, positioning it as a more dependable indicator of mantle fO_2 and as a tool for tracing the evolution of mantle fO_2 in terrestrial planets. In contrast, V/Ti and V/Yb are both more sensitive to the degree of melting and V/Ti is notably affected by mantle chemical composition. These insights refine our understanding of redox conditions across various tectonic environments on Earth. For instance, applying our model to data sets of primitive basalts reveals that the contemporary sub-arc mantle is generally more oxidised than the MORB mantle, consistent with impacts of slab-derived fluids and sediments in arc regions.

Received 18 July 2024 | Accepted 20 December 2024 | Published 7 February 2025

Introduction

The oxygen fugacity (fO_2) of Earth's mantle strongly influences crystallisation, magma composition and atmospheric evolution (Frost and McCammon, 2008; Evans, 2012; Stolper *et al.*, 2021). Directly measuring the upper mantle fO_2 is challenging because complexities introduced by partial melting, metasomatism and the scarcity of pristine samples obscure the prevailing fO_2 conditions (Frost and McCammon, 2008). Instead, primary melt $Fe^{3+}/\Sigma Fe$ ratios can be back calculated from basaltic glasses and coexisting mineral inclusions (Brounce *et al.*, 2014; Zhang *et al.*, 2018), though such measurements require access to facilities capable of Fe^{3+} analyses (Huang *et al.*, 2022) and the limited availability of reported Fe^{3+} contents that are accurate and thus suitable for comparison to geochemical models; *e.g.*, Fe^{3+} contents are reported for <3 % of mid-ocean ridge basalt (MORB) glasses in the PetDB database.

Vanadium is a multivalent (2+, 3+, 4+, 5+) element that, during partial mantle melting, exhibits variable mineral-melt partition coefficients (mineral D_i) that correlate with mantle fO_2. Consequently, the ratios of V to homovalent elements (*e.g.*, V/Sc, V/Ti, V/Yb) in primitive basalts have been employed to infer mantle fO_2 in various tectonic settings. Aside from temperature and pressure (*P*–*T*) (Wang *et al.*, 2019), the forward modelling approach using these ratios as oxybarometers relies on assumptions about mantle mineralogy and composition, as well as magmatic differentiation (Cottrell and Kelley, 2013; Laubier *et al.*, 2014; Nicklas *et al.*, 2019; Stolper and Bucholz, 2019; Gaborieau *et al.*, 2023). However, the exact mechanisms by which these parameters affect redox proxies in melts remain debated. V/Ti may be a more reliable indicator of mantle fO_2 than V/Sc because Sc behaves both compatibly and incompatibly in different mantle minerals, whereas Ti is consistently incompatible (Wang *et al.*, 2019; Gao *et al.*, 2022). Laubier *et al.* (2014) emphasised that V/Yb is less affected by magmatic differentiation. To explore how these redox proxies vary across mantle source lithologies and chemical compositions (Table 1), we here employed a non-modal partial melting model. For comparison, we independently simulated these redox sensitive ratios in the mantle sources of arc basalts and MORBs over the known mantle fO_2 range (see Supplementary Information for methods).

Results

Modelling the V-Sc-Ti-Yb system in the sub-arc mantle. Arc basalts form at pressures typical of the spinel stability field (Prytulak *et al.*, 2016). The presence of garnet in arc basalts is variable, however: it is unstable in basaltic magmas at 1.3 GPa and 900–1100 °C, but stable at 1.46 GPa and 1150 °C (Blatter *et al.*, 2023). Our compiled dataset reveals that while V/Sc ratios are relatively stable across natural abyssal and sub-arc peridotites, 100 × V/Ti and V/Yb ratios vary significantly (Fig. S-1; Supplementary Information). The depleted MORB mantle (DMM) and primitive mantle (PM) ratios for V/Sc (DMM, ~4.85; PM, ~5.24), 100 × V/Ti (DMM, ~9.90; PM, ~6.80) and V/Yb (DMM, ~197.50; PM, ~179.17) therefore serve as conservative initial compositions for our model.

Accordingly, we constructed models representing four sub-arc mineral assemblages and tested PM and DMM initial

1. Research Center for Earth and Planetary Material Sciences, School of Earth Sciences, Zhejiang University, Hangzhou, 310058, China
* Corresponding authors (email: c.-t.liu@zju.edu.cn; zhangzhou333@zju.edu.cn)

Table 1 Source mantle mineral assemblages and chemical compositions used to model the sub-arc and MORB mantle melting. PM, primitive mantle (Palme and O'Neill, 2014); DMM, depleted MORB mantle (Salters and Stracke, 2004). The petrological modelling is described in the Supplementary Information. Ol, olivine; Opx, orthopyroxene; Cpx, clinopyroxene; Spl, spinel; Amp, amphibole; Grt, garnet.

Source	Sub-arc mantle								MORB mantle			
Mineral assemblages	Spinel lherzolite[a]		Hydrous harzburgite[b]		Hydrous spinel harzburgite[c]		Garnet lherzolite[d]		Spinel lherzolite[c]		Fertile peridotite[e]	
Ol (wt. %)	57.0		58.0		58.0		53.1		57.0		51.0	
Opx (wt. %)	28.0		31.6		31.6		17.7		28.0		33.0	
Cpx (wt. %)	13.0		—		—		27.3		13.0		14.0	
Spl (wt. %)	2.0		—		2.0		—		2.0		2.0	
Amp (wt. %)	—		10.4		8.4		—		—		—	
Grt (wt. %)	—		—		—		3.0		—		—	
Chemical compositions	DMM	PM	DMM	PM	DMM	PM	DMM	PM	DMM	PM	DMM	PM
V (μg/g)	79	86	79	86	79	86	79	86	79	86	79	86
Ti (μg/g)	798	1265	798	1265	798	1265	798	1265	798	1265	798	1265
Sc (μg/g)	16.3	16.4	16.3	16.4	16.3	16.4	16.3	16.4	16.3	16.4	16.3	16.4
Yb (μg/g)	0.40	0.48	0.40	0.48	0.40	0.48	0.40	0.48	0.40	0.48	0.40	0.48
Figures	Fig. 1a–f		Fig. S-2a–f		Fig. S-2g–l		Fig. S-2m–r		Fig. 1g–l		Fig. S-3a–f	

a: from Workman and Hart (2005).
b: from Lara and Dasgupta (2020).
c: modified from Lara and Dasgupta (2020).
d: from Walter (1998).
e: from Borghini *et al.* (2013).

chemical compositions for each assemblage (Table 1, Fig. 1a–f; Supplementary Information). Although mineral D_i values can evolve over a wide range, the bulk D_i tends to be more stable. For example, although Sc is variously compatible or incompatible in different mantle minerals (Wang *et al.*, 2019), our petrological modelling indicates that Sc is predominantly incompatible during mantle melting (Fig. 1b,h). Nonetheless, Sc is less incompatible than Ti and Yb in all modelled arc mantle mineral assemblages (Figs. 1, S-2).

In contrast to these homovalent elements, mantle fO_2 strongly influences V partitioning. Our modelling results indicate that V remains incompatible at ΔFMQ = 0 to ΔFMQ +2 (oxygen fugacity reported in log units relative to the fayalite-magnetite-quartz oxygen buffer). However, V can become compatible at low degrees of partial melting at ΔFMQ −2 (Fig. 1c). In hydrous harzburgite and hydrous spinel harzburgite, V is mainly incompatible (Fig. S-2c,i). In comparison, V is increasingly incompatible during partial melting in lithologies containing increased proportions of olivine (Ol; Fig. 1c) because V is highly incompatible in Ol. Given the diverse mineral assemblages and compositions we explored, V/Sc in the melt remains relatively stable between ΔFMQ −2 and ΔFMQ = 0, although values increase slightly at increased degrees of melting (Fig. 1d). In contrast, V/Sc ratios are much higher in melts produced by lower degrees of melting at ΔFMQ +2 (Fig. 1d).

V/Ti (here reported as 100 × V/Ti; Figs. 1e, S-2e,k,h) and V/Yb (Figs. 1f, S-2l,h,r) are sensitive to the degree of partial melting and fO_2 conditions, but are relatively insensitive to mineral assemblages. V/Ti is particularly affected by the initial chemical (PM *vs.* DMM) composition; for example, after 15 % melting of spinel lherzolite at ΔFMQ +2, the melts with DMM and PM initial chemical compositions have 100 × V/Ti ≈ 7.35 and 5.05, respectively, differing by about a factor of 1.5 (Fig. 1e).

Modelling the V-Sc-Ti-Yb system in the MORB mantle. MORBs typically form within the spinel stability field (Lee *et al.*, 2005). We modelled both PM and DMM initial compositions for two MORB mantle mineral assemblages (Table 1, Fig. 1g–l; Supplementary Information). In these assemblages, Sc, Yb and Ti are always incompatible, becoming increasingly so at high degrees of partial melting (Figs. 1h, S-3b); Yb and Ti are more incompatible than Sc. V also remains incompatible between ΔFMQ −2 and ΔFMQ +2 (Figs. 1i, S-3c). V/Sc remains nearly constant during partial melting between ΔFMQ −2 and ΔFMQ = 0 for both considered source lithologies and chemical compositions (Figs. 1j, S-3d), but gradually decreases with increasing degree of melting at ΔFMQ +2.

V/Ti is particularly sensitive to the degree of partial melting and chemical composition, but less sensitive to mineral assemblage (Figs. 1k, S-3e). For instance, 10 % melting of spinel lherzolite with DMM or PM composition at ΔFMQ +2 produces melt with 100 × V/Ti ≈ 7.87 or 5.41, respectively, again differing by a factor of almost 1.5 (Fig. 1e). V/Yb is not greatly influenced by mineral assemblage or chemical composition (Figs. 1l, S-3f), although it increases with increased degree of melting from ΔFMQ −2 to ΔFMQ = 0 but decreases with increased degree of melting at ΔFMQ +2.

Discussion

Comparison of the V-Sc-Ti-Yb system with source characteristics and partial melting. Our results show that V/Sc remains relatively stable during the partial melting of various mantle sources at ΔFMQ −2 to ΔFMQ = 0. This stability is attributed to the similar bulk D values of Sc and V during melting (*e.g.*, Fig. 1b,c,h,i). The slight increase of V/Sc during melting at those fO_2 conditions is due to the moderate increase in the incompatibility of V (*e.g.*, Fig. 1b,h). At ΔFMQ +2, however, V/Sc tends to decrease during partial melting due to the higher incompatibility of V than Sc (*e.g.*, Fig. 1b–d,h–j). Nonetheless, the changes in V/Sc are modest and may not be drastically affected by typical degrees of melting in parental arc magmas (~10–20 %) or primary

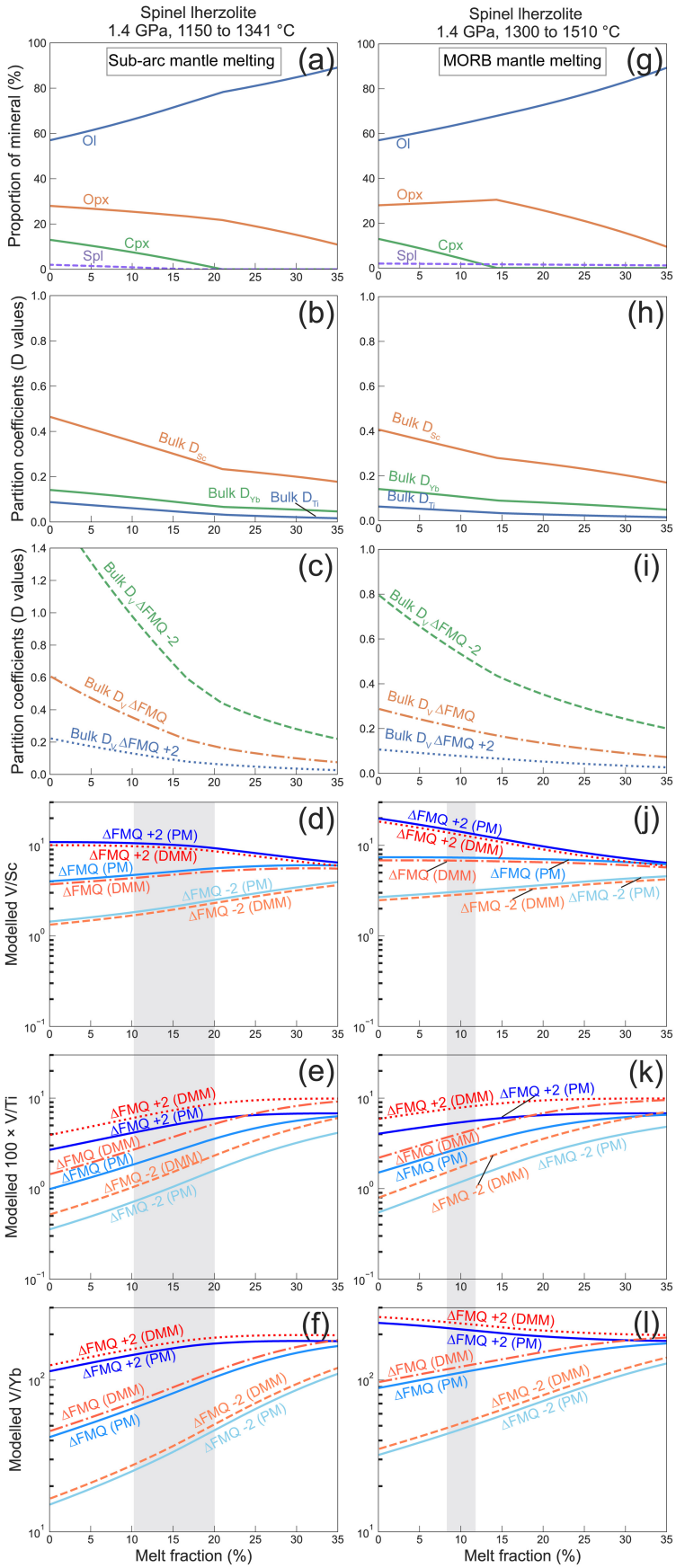

Figure 1 Modelling results for **(a–f)** sub-arc and **(g–l)** MORB mantle melting (see Table 1). Variations in modelled **(a, g)** mineral proportions and **(b, c, h, i)** bulk partition coefficients (*D*) for V, Sc, Ti and Yb are shown, as well as **(d–f, j–l)** ratios of V/Sc, 100 × V/Ti and V/Yb during partial melting of DMM and PM chemical compositions. Abbreviations are as defined in Table 1.

MORB melts (~10 %) (Lee *et al.*, 2005; Prytulak *et al.*, 2016). V/Sc is largely unaffected by mineral assemblage and chemical composition because the bulk D_{Sc} values are consistent across the considered lithologies (*e.g.*, Figs. 1b, S-2b,h,t) and because the mantle compositions have similar initial V/Sc (Table 1).

The 100 × V/Ti ratio increases with increasing degree of partial melting primarily because Ti is more incompatible than V (*e.g.*, Fig. 1b,c,h,i). Moreover, 100 × V/Ti is sensitive to chemical composition due to the variability of Ti contents in the mantle compositions (Table 1). Our results also suggest that V/Ti in the melt is more sensitive to initial chemical composition under more oxidising conditions (*e.g.*, Fig. 1e,k), which we attribute to the greater incompatibility of V, and thus greater enrichment of V in the melt, compared to more reducing conditions. All else being equal, any significant change of V/Ti in the mantle source will be amplified in the melt.

Except in the MORB mantle under oxidising conditions, V/Yb increases during partial melting, mainly because Yb is more incompatible than V (*e.g.*, Fig. 1b,c,h,i). V/Yb varies among lithological sources but is not greatly impacted by chemical composition due to the consistent Yb contents of the different sources (Table 1).

Accordingly, in the context of a complex mantle mineralogy and source composition, our simplified petrological model indicates that V/Sc is a more reliable indicator of mantle redox conditions than V/Ti or V/Yb. Furthermore, compared to $Fe^{3+}/\Sigma Fe$ analyses in mineral inclusions, it is more feasible to obtain V and Sc data for basalts. Therefore, considering secular changes in mantle melting and chemical composition (Herzberg *et al.*, 2010; Keller and Schoene, 2012), V/Sc in primary basaltic melts is a robust redox proxy useful for tracing the evolution of mantle fO_2, which can provide valuable insights into the redox histories of the Earth and other terrestrial planets.

Oxygen fugacities of sub-arc and MORB mantle sources. To reconstruct the mantle fO_2 in different tectonic settings, it is imperative to ascertain both the redox proxy values (*e.g.*, V/Sc) of primitive basalts and the *P*–*T* conditions at which their parental magmas melted (Lee *et al.*, 2009). We compiled a global suite of modern arc basalts and MORBs from the GEOROC and PetDB databases (see Supplementary Information). Additionally, to compare with fO_2 values derived from Fe-XANES data sets (Brounce *et al.*, 2014; Birner *et al.*, 2018), we collected basalt samples from the Guguan volcanoes in the Mariana arc and from the central Southwest Indian Ridge (SWIR) from the GEOROC and PetDB databases (see Supplementary Information).

The crystallisation of magnetite and ilmenite reduces V and Ti concentrations in magmas, while clinopyroxene precipitation decreases Sc concentrations (Li and Lee, 2004). We, therefore, selected primitive samples with 8–12 wt. % MgO to minimise the impacts of mineral crystallisation/accumulation (see Supplementary Information; Figs. S-10, S-11). By integrating these data with our petrological modelling, we converted V/homovalent element ratios to mantle fO_2.

Oxygen fugacity of the modern sub-arc mantle. We assumed mean melting conditions of 1.4 GPa and 1260 °C for the sub-arc mantle (Fig. S-10d) and plotted V/homovalent element ratios against fO_2 for spinel lherzolite, hydrous harzburgite and hydrous spinel harzburgite lithologies with PM or DMM chemical compositions (Figs. 2a,b, S-12 to S-14). Furthermore, we also considered the V/Sc-fO_2 relationship during garnet lherzolite melting at 3.0 GPa and 1260 °C. Additionally, we simulated melting conditions of 1.0 GPa and 1219 °C for the Mariana (Guguan) arc mantle (Fig. S-11d) and plotted V/homovalent element ratios *versus* fO_2 for spinel lherzolite with PM or DMM chemical compositions (Figs. 2e,f, S-15).

By applying the average V/Sc, 100 × V/Ti and V/Yb ratios of primitive arc basalts to these V/homovalent element-fO_2 curves, we estimated average fO_2 values and their associated 1 s.d. uncertainties in various mantle source mineral assemblages and compositions (Figs. 3, S-12 to S-15). The consistency of the modelled arc mantle fO_2 values within the error range across this spectrum underscores the reliability of V/Sc as an indicator of arc mantle fO_2 (Figs. 2a,b,e,f, 3a). The mean global sub-arc mantle fO_2 value is ΔFMQ +1.36 ± 0.68 (2 standard error of the mean; 2 s.e.m.; $n = 895$) across the considered mineral assemblages and chemical compositions (Fig. 3a). Moreover, the estimated Mariana (Guguan) arc mantle fO_2 values are ΔFMQ +1.06 ± 0.13 (DMM) and ΔFMQ +0.86 ± 0.13 (PM) ($n = 10$) (Fig. 2e,f), consistent with fO_2 values of ΔFMQ +1.0 to ΔFMQ +1.6 derived from the $Fe^{3+}/\Sigma Fe$ ratios of melt inclusions in Mariana arc basalts (Brounce *et al.*, 2014) (Fig. 3a).

Oxygen fugacity of the modern MORB mantle. We considered mean melting conditions of 1.4 GPa and 1375 °C for the MORB mantle and plotted V/Sc, 100 × V/Ti and V/Yb ratios *versus* fO_2 for spinel lherzolite and fertile peridotite with PM and DMM chemical compositions (Figs. 2c,d, S-16 to S-18). Using the mean V/Sc, 100 × V/Ti and V/Yb ratios of global primitive MORBs and these V/homovalent element-fO_2 curves, we estimated average fO_2 values and associated 1 s.d. uncertainties across various mantle source mineral assemblages and compositions (Fig. 3). Furthermore, we modelled melting conditions of 1.5 GPa and 1279 °C for the SWIR mantle (Fig. S-11d) and plotted V/homovalent element ratios *versus* fO_2 for spinel lherzolite with PM or DMM chemical compositions (Figs. 2g,h, S-19).

Again, the consistency of our results within uncertainties reflects the reliability of V/Sc as an indicator of MORB mantle fO_2. Our estimate of the mean MORB mantle fO_2 value is ΔFMQ 0.00 ± 0.35 (2 s.e.m., $n = 859$) across the considered mineral assemblages and chemical compositions (Fig. 3a). Our findings are consistent with previously reported mean fO_2 values determined from $Fe^{3+}/\Sigma Fe$ ratios in MORB glasses (ΔFMQ +0.10 ± 0.18, 1 s.d., $n = 103$, Cottrell and Kelley, 2011; ΔFMQ –0.18 ± 0.16, 1 s.d., $n = 13$, Zhang *et al.*, 2018) and using the V-in-Ol method (ΔFMQ –0.28 ± 0.28, 2 s.d., $n = 8$, Nicklas *et al.*, 2024). Our evaluated SWIR mantle fO_2 values are ΔFMQ –0.01 ± 0.48 (DMM) and ΔFMQ –0.29 ± 0.45 (PM) ($n = 10$) (Fig. 2g,h). These results are consistent with average MORB mantle fO_2 values of ΔFMQ –0.16 ± 0.13 (1 s.d., $n = 31$) and ΔFMQ 0.00 ± 0.72 (1 s.d., $n = 41$) determined for primary MORB glasses and peridotites from the SWIR, respectively (Birner *et al.*, 2018) (Fig. 3a).

V/Ti and V/Yb are less sensitive to mantle fO_2. In contrast to the results obtained using V/Sc, the estimated average fO_2 values for the global sub-arc and MORB mantle determined using V/Ti span wide ranges, with mean values of ΔFMQ −0.28 ± 1.62 and ΔFMQ −0.79 ± 1.24 (2 s.e.m.), respectively (Fig. 3b). Similarly, the average fO_2 values estimated for the Guguan arc and the SWIR mantle from V/Ti also exhibit significant variability (Figs. S-15, S-19). These substantial variations can be attributed to the sensitivity of V/Ti to mantle composition (Fig. 1e,k). Additionally, the mean values of global sub-arc and MORB mantle fO_2 estimated by V/Yb are ΔFMQ +0.28 ± 0.80 and ΔFMQ −1.03 ± 0.24 (2 s.e.m.), respectively (Fig. 3c). Generally, the mean mantle fO_2 values derived using V/Ti and V/Yb are significantly lower than those derived from V/Sc, likely due to the strong incompatibilities of Ti and Yb during partial melting; this ultimately leads to an underestimation of mantle fO_2 due to the lower V/Ti and V/Yb values in the melts.

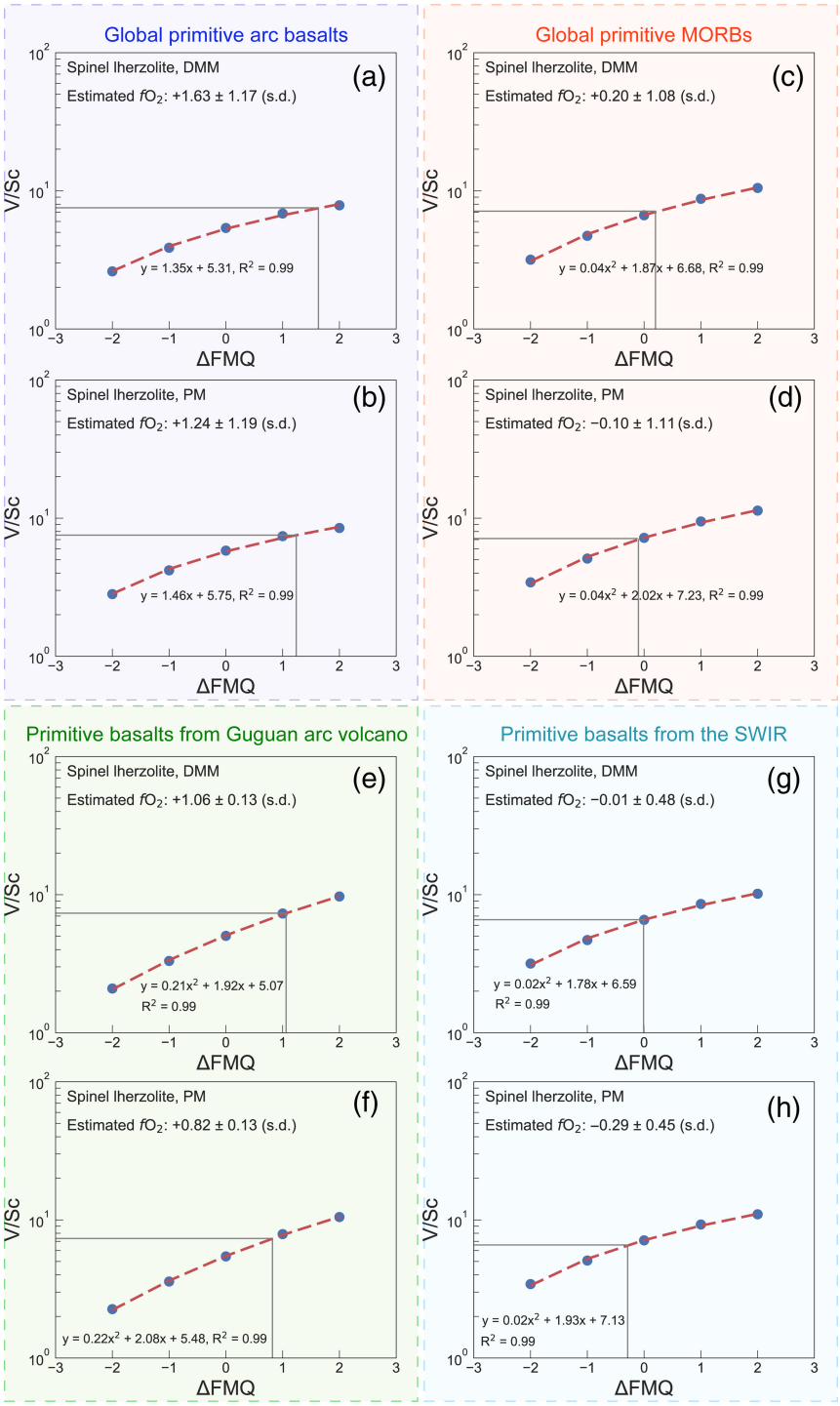

Figure 2 Modelled V/Sc ratios in **(a, b)** arc magmas, **(c, d)** MORB, **(e, f)** Guguan volcano (Marian arc) and **(g, h)** the Southwest Indian Ridge (SWIR) magmas *versus* fO_2 in spinel lherzolite with DMM or PM chemical compositions. Dashed lines represent fitted curves. Mean fO_2 values (with 1 s.d. uncertainties) were estimated from the V/Sc-fO_2 curves and the average V/Sc ratios in primitive basalts. The horizontal and vertical grey lines show the average V/Sc ratios and calculated fO_2 values, respectively.

Implications

Previous studies indicated that the comparable V/Sc ratios in primitive arc basalts and MORBs suggest comparable fO_2 conditions in their mantle sources (*e.g.*, Lee *et al.*, 2005). However, a recent experimental study showed that D_V/D_{Sc} values are higher at low temperatures than at high temperatures for a given fO_2, resulting in lower V/Sc ratios in melts produced at lower temperatures (Wang *et al.*, 2019). By comparing Figure 1d and 1j at a given melt fraction, it is evident that the competing effects of T and fO_2 can lead to similar V/Sc in melts from differently oxidised mantle sources. In other words, arc magmas generated from lower temperatures but higher fO_2 than MORB melts could still exhibit comparable V/Sc ratios to MORBs. Our petrological modelling suggests that the sub-arc mantle fO_2 is, on average, more oxidised than that of the MORB mantle source (Fig. 3a). This finding aligns with estimations based on Cu/Zr-Zr in primary arc and MORB magmas (Zhao *et al.*,

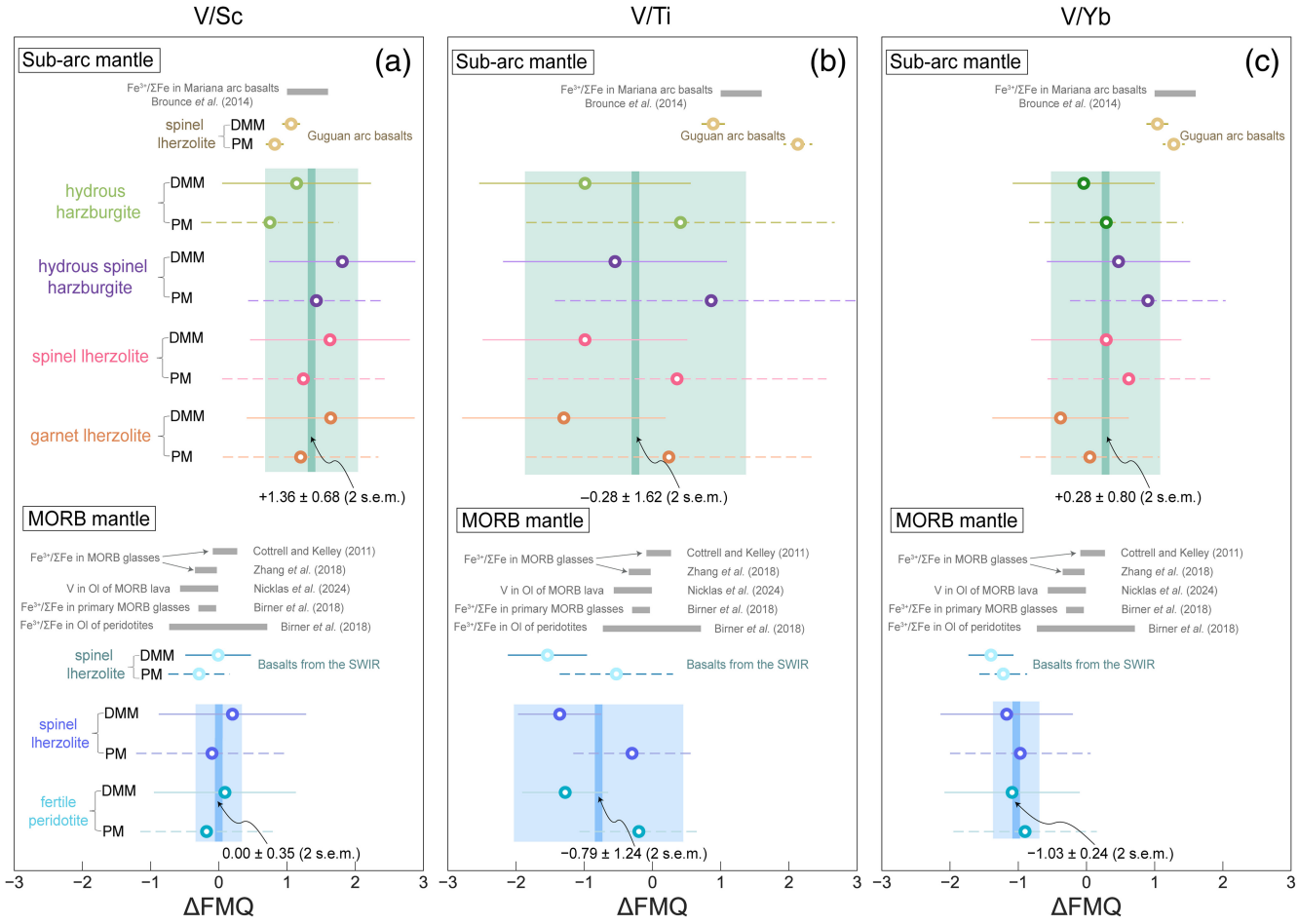

Figure 3 Average sub-arc and MORB mantle fO_2 values estimated *via* **(a)** V/Sc, **(b)** 100 × V/Ti and **(c)** V/Yb across the considered source mineral assemblages and chemical compositions (Supplementary Information). Horizontal error bars show 1 s.d. uncertainties. The vertical green and blue colour bands illustrate the mean estimated values of global sub-arc and MORB mantle fO_2 with 2 s.e.m. errors. The grey horizontal bands show ranges of previously determined sub-arc and MORB mantle fO_2 values.

2022), which is expected given the influence of slab-derived fluids and sediments (Brounce *et al.*, 2014; Bénard *et al.*, 2018).

Author Contributions

JZZ and CTL collectively designed this research. CTL compiled the dataset and implemented the modelling. CTL wrote the original draft with contributions from CYY and JZZ.

Data Availability Statement

The data needed to evaluate the conclusions in this study are archived at Zenodo and are currently available at https://doi.org/10.5281/zenodo.14642336.

Acknowledgements

This study was funded by NSFC (grant No. 42072066). We thank C.-G. Sun for the fruitful discussion and R. Dennen for polishing the manuscript. We thank J.-T. Wang for the clarification of his petrological model. We acknowledge very constructive reviews by Maryjo Brounce, Robert Nicklas and Veronique Le Roux. We thank Horst R. Marschall for his careful editorial handling.

Editor: Horst R. Marschall

Additional Information

Supplementary Information accompanies this letter at https://www.geochemicalperspectivesletters.org/article2504.

Cite this letter as: Liu, C.-T., Ye, C.-Y., ZhangZhou, J. (2025) Modelling redox state *via* V-Sc-Ti-Yb partitioning in mantle derived melts. *Geochem. Persp. Let.* 33, 56–62. https://doi.org/10.7185/geochemlet.2504

References

Bénard, A., Klimm, K., Woodland, A.B., Arculus, R.J., Wilke, M., Botcharnikov, R.E., Shimizu, N., Nebel, O., Rivard, C., Ionov, D.A. (2018) Oxidising agents in sub-arc mantle melts link slab devolatilisation and arc magmas. *Nature Communications* 9, 3500. https://doi.org/10.1038/s41467-018-05804-2

Birner, S.K., Cottrell, E., Warren, J.M., Kelley, K.A., Davis, F.A. (2018) Peridotites and basalts reveal broad congruence between two independent records of mantle fO_2 despite local redox heterogeneity. *Earth and Planetary Science Letters* 494, 172–189. https://doi.org/10.1016/j.epsl.2018.04.035

Blatter, D.L., Sisson, T.W. Hankins, W.B. (2023) Garnet stability in arc basalt, andesite, and dacite—an experimental study. *Contributions to Mineralogy and Petrology* 178, 33. https://doi.org/10.1007/s00410-023-02008-w

Borghini, G., Rampone, E., Zanetti, A., Class, C., Cipriani, A., Hofmann, A.W., Goldstein, S.A. (2013) Meter-scale Nd isotopic heterogeneity in pyroxenite-bearing Ligurian peridotites encompasses global-scale upper mantle variability. *Geology* 41, 1055–1058. https://doi.org/10.1130/g34438.1

Brounce, M.N., Kelley, K.A., Cottrell, E. (2014) Variations in $Fe^{3+}/\Sigma Fe$ of Mariana Arc Basalts and Mantle Wedge fO_2. *Journal of Petrology* 55, 2513–2536. https://doi.org/10.1093/petrology/egu065

Cottrell, E., Kelley, K.A. (2011) The oxidation state of Fe in MORB glasses and the oxygen fugacity of the upper mantle. *Earth and Planetary Science Letters* 305, 270–282. https://doi.org/10.1016/j.epsl.2011.03.014

Cottrell, E., Kelley, K.A. (2013) Redox Heterogeneity in Mid-Ocean Ridge Basalts as a Function of Mantle Source. *Science* 340, 1314–1317. https://doi.org/10.1126/science.1233299

Evans, K.A. (2012) The redox budget of subduction zones. *Earth-Science Reviews* 113, 11–32. https://doi.org/10.1016/j.earscirev.2012.03.003

Frost, D.J., McCammon, C.A. (2008) The Redox State of Earth's Mantle. *Annual Review of Earth and Planetary Sciences* 36, 389–420. https://doi.org/10.1146/annurev.earth.36.031207.124322

Gaborieau, M., Laubier, M., Pompilio, M., Bolfan-Casanova, N. (2023) Determination of the oxidation state of primary melts using two proxies. *Chemical Geology* 638, 121701. https://doi.org/10.1016/j.chemgeo.2023.121701

Gao, L., Liu, S., Cawood, P.A., Hu, F., Wang, J., Sun, G., Hu, Y. (2022) Oxidation of Archean upper mantle caused by crustal recycling. *Nature Communications* 13, 3283. https://doi.org/10.1038/s41467-022-30886-4

Herzberg, C., Condie, K., Korenaga, J. (2010) Thermal history of the Earth and its petrological expression. *Earth and Planetary Science Letters* 292, 79–88. https://doi.org/10.1016/j.epsl.2010.01.022

Huang, W., Lyu, Y., Du, M., He, C., Gao, S., Xu, R., Xia, Q., ZhangZhou, J. (2022) Estimating ferric iron content in clinopyroxene using machine learning models. *American Mineralogist* 107, 1886–1900. https://doi.org/10.2138/am-2022-8189

Keller, C.B., Schoene, B. (2012) Statistical geochemistry reveals disruption in secular lithospheric evolution about 2.5 Gyr ago. *Nature* 485, 490–493. https://doi.org/10.1038/nature11024

Lara, M., Dasgupta, R. (2020) Partial melting of a depleted peridotite metasomatized by a MORB-derived hydrous silicate melt – Implications for subduction zone magmatism. *Geochimica et Cosmochimica Acta* 290, 137–161. https://doi.org/10.1016/j.gca.2020.09.001

Laubier, M., Grove, T.L., Langmuir, C.H. (2014) Trace element mineral/melt partitioning for basaltic and basaltic andesitic melts: An experimental and laser ICP-MS study with application to the oxidation state of mantle source regions. *Earth and Planetary Science Letters* 392, 265–278. https://doi.org/10.1016/j.epsl.2014.01.053

Lee, C.-T.A., Leeman, W.P., Canil, D., Li, Z.-X.A. (2005) Similar V/Sc systematics in MORB and arc basalts: Implications for the oxygen fugacities of their mantle source regions. *Journal of Petrology* 46, 2313–2336. https://doi.org/10.1093/petrology/egi056

Lee, C.-T.A., Luffi, P., Plank, T., Dalton, H., Leeman, W.P. (2009) Constraints on the depths and temperatures of basaltic magma generation on Earth and other terrestrial planets using new thermobarometers for mafic magmas. *Earth and Planetary Science Letters* 279, 20–33. https://doi.org/10.1016/j.epsl.2008.12.020

Li, Z.-X.A., Lee, C.-T.A. (2004) The constancy of upper mantle fO_2 through time inferred from V/Sc ratios in basalts. *Earth and Planetary Science Letters* 228, 483–493. https://doi.org/10.1016/j.epsl.2004.10.006

Nicklas, R.W., Puchtel, I.S., Ash, R.D., Piccoli, P.M., Hanski, E., Nisbet, E.G., Waterton, P., Pearson, D.G., Anbar, A.D. (2019) Secular mantle oxidation across the Archean-Proterozoic boundary: Evidence from V partitioning in komatiites and picrites. *Geochimica et Cosmochimica Acta* 250, 49–75. https://doi.org/10.1016/j.gca.2019.01.037

Nicklas, R.W., Puchtel, I.S., Baxter, E.F. (2024) Concordance of V-in-olivine and Fe-XANES oxybarometry methods in mid-ocean ridge basalts. *Earth and Planetary Science Letters* 625, 118492. https://doi.org/10.1016/j.epsl.2023.118492

Palme, H, O'Neill, H.St.C. (2014) 3.1 – Cosmochemical Estimates of Mantle Composition. In: Holland, H.D., Turekian, K.K. (Eds.) *Treatise on Geochemistry*. Second Edition, Elsevier, Oxford, 1–35. https://doi.org/10.1016/B978-0-08-095975-7.00201-1

Prytulak, J., Sossi, P.A., Halliday, A.N., Plank, T., Savage, P.S., Woodhead, J.D. (2016) Stable vanadium isotopes as a redox proxy in magmatic systems? *Geochemical Perspectives Letters* 3, 75–84. https://doi.org/10.7185/geochemlet.1708

Salters, V.J.M., Stracke, A. (2004) Composition of the depleted mantle. *Geochemistry, Geophysics, Geosystems* 5, Q05B07. https://doi.org/10.1029/2003GC000597

Stolper, D.A., Bucholz, C.E. (2019) Neoproterozoic to early Phanerozoic rise in island arc redox state due to deep ocean oxygenation and increased marine sulfate levels. *Proceedings of the National Academy of Sciences* 116, 8746–8755. https://doi.org/10.1073/pnas.1821847116

Stolper, D.A., Higgins, J.A., Derry, L.A. (2021) The role of the solid earth in regulating atmospheric O_2 levels. *American Journal of Science* 321, 1381–1444. https://doi.org/10.2475/10.2021.01

Wang, J., Xiong, X., Takahashi, E., Zhang, L., Li, L., Liu, X. (2019) Oxidation State of Arc Mantle Revealed by Partitioning of V, Sc, and Ti Between Mantle Minerals and Basaltic Melts. *Journal of Geophysical Research: Solid Earth* 124, 4617–4638. https://doi.org/10.1029/2018jb016731

Walter, M.J. (1998) Melting of Garnet Peridotite and the Origin of Komatiite and Depleted Lithosphere. *Journal of Petrology* 39, 29–60. https://doi.org/10.1093/petrology/39.1.29

Workman, R.K., Hart, S.R. (2005) Major and trace element composition of the depleted MORB mantle (DMM). *Earth and Planetary Science Letters* 231, 53–72. https://doi.org/10.1016/j.epsl.2004.12.005

Zhang, H.L., Cottrell, E., Solheid, P.A., Kelley, K.A., Hirschmann, M.M. (2018) Determination of $Fe^{3+}/\Sigma Fe$ of XANES basaltic glass standards by Mössbauer spectroscopy and its application to the oxidation state of iron in MORB. *Chemical Geology* 479, 166–175. https://doi.org/10.1016/j.chemgeo.2018.01.006

Zhao, S.-Y., Yang, A.Y., Langmuir, C.H., Zhao, T.-P. (2022) Oxidized primary arc magmas: Constraints from Cu/Zr systematics in global arc volcanics. *Science Advances* 8, eabk0718. https://doi.org/10.1126/sciadv.abk0718